Growth Kinetics of Gold Nanoparticles in Reverse Micelles

A.P. Herrera*, E. Vicu a*, C. Rinaldi*, M. Castro**, L. Sol ***, R. Irizarry*** and J.G. Briano*

*Chemical Engineering Department, University of Puerto Rico
Mayagüez PR 00680, crinaldi@uprm.edu, jbriano@uprm.edu.
**Chemistry Department, University of Puerto Rico
Mayagüez PR 00680, mcastro@uprm.edu.
*** DuPont Electronics Microcircuits Industries, Ltd.
Manatí PR 00674-3000, Roberto.Irizarry@PRI.dupont.com.

ABSTRACT

Gold nanoparticles were formed from the reduction of gold (III) by sulfite in reverse micelles and monitored with a stopped flow analyzer. The gold and the reducing agent micelles were formed in isooctane and AOT (as surfactant). The overall reduction of gold (III) occurred in less than 20 [ms]. The growth kinetics was followed from measurements of the time-dependent wavelength absorption spectra, and by analyzing the evolution of the dipole resonance. The dielectric constant of the medium was calculated, and the growth results were modeled with Mie's scattering theory. The modeling assumes the mean size of the particles to be characterized by the position of the plasmon. Excellent agreement between theory and experiment are found at the peak maximum and long wavelength tail, for particle sizes up to 90 [nm]. The dependence of the gold dielectric constant on particle size and the effect of multi-pole interactions were taken into consideration.

Keywords: micelles, growth kinetics, gold nanoparticles

REVERSE MICELLES

A wide range of techniques for the synthesis and characterization of gold nanoparticles have been developed in the past years with the objective of controlling the size and shape of the resulting nanoparticles. Examples include reduction of Au^{+3} in aqueous solution [1, 2], ultrasonic mixing of the reactants [3], ultraviolet photo-activation techniques [4], and preparation in reverse micelles [5-10], among others. Characterization of the resulting nanoparticles can be performed using UV-VIS absorption spectroscopy, Transmission Electron Microscopy (TEM), and also Surface Second Harmonic Generation (SSHG).

Reverse micelles consist of aqueous nanometer-sized droplets that are separated from the bulk organic phase by a surfactant layer (figure 1). This is an isotropic and thermodynamically stable single-phase system that consists of three components: water, organic solvent, and surfactant [11].

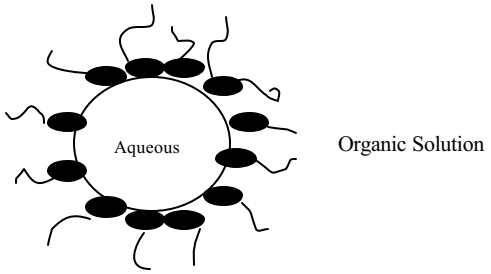

Figure 1: Illustration of a reverse micelle.

A surfactant molecule lowers the interfacial tension between water and oil resulting in the formation of a transparent solution as the two phases intermingles. Using reverse micelles for nanostructure synthesis takes advantage of the small size of the micellar water pools, which essentially act as nanoreactors. These nanoreactors collide continuously due to thermal Brownian motion, hence a small fraction of droplets exist in the form of short-lived dimmers which exchange their water content. After a short time these dimmers separate to form two droplets (as illustrated in Figure 2). As a result of this coalescence and separation mechanism, molecules in the water pools are redistributed over the micellar population [12].

The size of the water pool inside the reverse micelle greatly influences the size of the resulting nanoparticles. Thus, changing the size of the water pool provides a mechanism to control the final nanoparticle size [13]. The final size of the water pool has been described to depend on the water-surfactant molar ratio, $w = [H_2O]/[AOT]$. In order to obtain reverse micelles in the water/AOT system, this ratio must be below 15 [14, 15]. By using Aerosol OT [Sodium bis(2ethylhexyl) sulfosuccinate], Na(AOT), as the surfactant, and isooctane as solvent, it has been demonstrated that the water pool diameter R is related to the water content w of the droplet by [14, 15]:

$$R_w \quad 3V_{Aq}\frac{H_2O}{S} \qquad (1)$$

Where V_{Aq} is the volume of water molecules, s is the area per polar head, and S is the concentration of the surfactant AOT. With the definition w = [H_2O]/[AOT], equation (1) can be expressed in the form:

$$R_w(\text{Å}) \quad 1.5w \qquad (2)$$

As illustrated in Figure 2, synthesis of nanoparticles by using reverse micelles, involves the preparation of two identical water-in-oil microemulsions. Reactants A and B, are dissolved in the aqueous phases of these two microemulsions. Upon mixing, collisions and droplet coalescence bring the reactants A and B into contact to form the AB precipitate. This precipitate is confined to the interior of the reverse micelle droplets and the size and shape of the particle formed reflects the interior of the droplet [16]. Since the compositions of the two microemulsions (I and II) are identical, differing only in the nature of the aqueous phase, the microemulsion is not destabilized upon mixing. One of the disadvantages of using this method is that it is necessary to use large quantities of solvent and surfactant to produce a relatively small amount of nanoparticles. Also, the formation of the reverse micelle depends on many factors including temperature, mixing time, mixing type and order, and the way in which precursors are added to the reaction vessel.

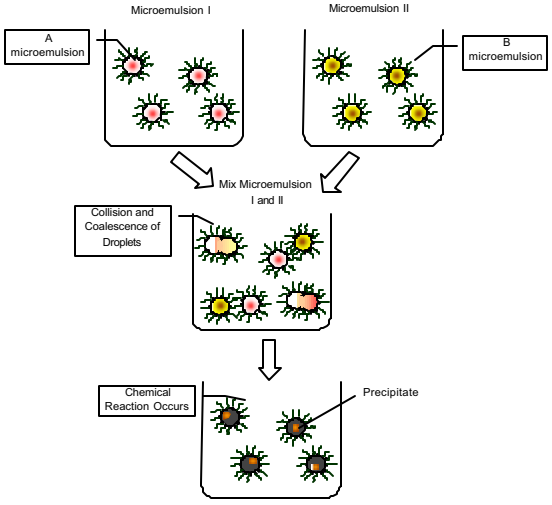

Figure 2: Schematic representation of synthesis of nanoparticles in reverse micelle.

OPTICAL PROPERTIES

Optical properties of gold nanoparticles have been intensively investigated during recent years, particularly their dependence on size [1, 2]. Absorption spectra of colloidal dispersions of metals exhibit broad regions in the UV-Visible range due to the excitation of the plasmon resonance or inter-band transitions, characteristic of the metallic properties of the material [17]. The UV-Visible absorption spectra of a fairly dilute dispersion of colloidal particles can be calculated from Mie's Theory [2, 18, 19]. This theory was developed for a single spherical particle, assuming the dielectric constant to be independent of the particle size [18].

The extinction coefficient C_{ext} is related to the Mie scattering coefficients a_n and b_n through

$$C_{ext} \quad \frac{2}{x^2} \sum_{n\ 1}^{\infty} (2n \quad 1)[\text{Re}(a_n \quad b_n] \qquad (3)$$

where x = $dn_0/$, n_0 is the refractive index of the host medium, is the wavelength of the incident light *in vacuo*. a_n and b_n are the scattering coefficients, which are functions of the particle diameter, d, and of the wavelength in terms of Ricatti-Bessel functions. For particles with diameters less than 100 [nm], only the first three terms in equation (3) are usually needed. In the case of gold, an excellent agreement is obtained for particle sizes higher than 40nm in aqueous medium The discrepancy for smaller sizes is due to the unknown dependency of the dielectric constant with size. The position of the maximum absorption is directly related [1, 2] to the mean size of the particles as showed on Figure 3. Our experimental data were obtained from commercial colloids which have narrow size distributions, but important enough to explain any deviations from Mie's model.

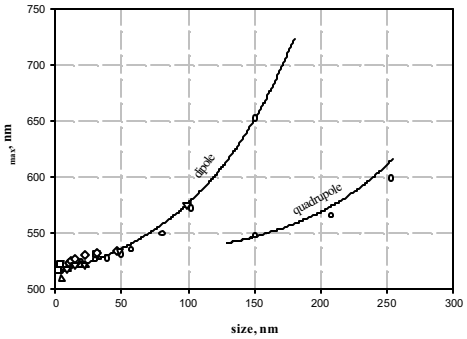

Figure 3. Position of the maximum absorption peak, versus particle size, for gold particles in aqueous medium. The solid lines are simulations using Mie's equation and the symbols are absorption measurements. Experimental data is shown as: squares [Galleto, P., et al., 1999 [20]], triangles up [Logunov, S.T., et al., 1997 [21]], triangles down [Stephan, L., and M. A. El-Sayed, 1999 [22]], diamonds [Sau, T.K., et al., 2001 [23]], and circles [Viera, O., 2002 [24]].

When using micelles, the optical properties of the metallic particle will be influenced by the dielectric function of the medium which depends on the nature of the organic solvent, and of the surfactant, as well as on the size of the micelles. To estimate the effect of the dielectric

constant on the position of the plasmon resonance, we prepared reverse micelles using commercial gold colloids at *w* ranging from 5 to 20. Our preliminary study on this effect is summarized on Figure 4, where the shift in the plasmon position may be seen as function of *w*.

In this preliminary study, we see that the plasmon peak seems to move to the lower energy range as the micelles get smaller. For $w = 5$, there is a shift of about 9 nm to the right for all particle sizes. As micelles get larger, the optical properties approach that of the aqueous medium case.

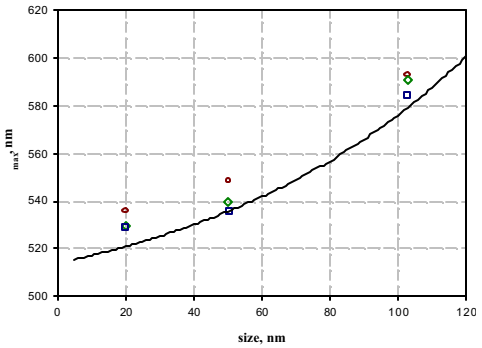

Figure 4. Position of the maximum absorption peak versus particle size of gold particles, in reverse micelles. The solid line is a numerical simulation using Mie's equation for aqueous medium. Small circles correspond to $w = [H_2O]/[AOT] = 5$, diamonds to $w = 10$, and squares to $w = 15$.

GROWTH KINETICS

L.E Murillo et al [1] have studied the formation of gold nanoparticles from aqueous solution by reducing $AuCl_4$ with sulfite, the reduction/nucleation/growth process took less than 1 s, and required a particularly fast technique to follow the optical changes; for this reason, a Stopped Flow Reactor (SFR) was used. In this work, the specific optical properties of the metallic particles, and the gold plasmon resonance were followed in the range of 10 to 100 nm, by using Mie's theory, as developed for a single spherical particle.

A typical time dependent spectrum for reduction and growth of nano-sized gold particles is presented in Figure 5. The initial reduction stage is characterized by the depletion of the 300 nm band (characteristic of gold III). Complete reduction of gold (III) was obtained in 15 ms. Plasmon resonance due to metallic behavior is associated with the peak in the 500 nm region. Figure 7, shows the computation of size evolution assuming the suspension to be statistically narrow [2].

To follow the formation of gold nanoparticles into reverse micelles, we used the same equipment than for the aqueous medium case. Since the system is confined into these "nanoreactors", the process is slower and the particles growth up to a given smaller size. In fact, we were able to stabilize gold particles of any size by just changing *w*, or the relative concentrations of the reactants.

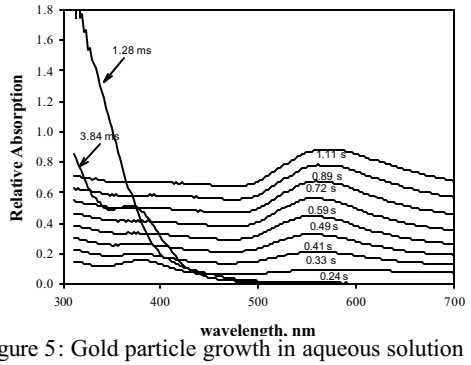

Figure 5: Gold particle growth in aqueous solution [1]

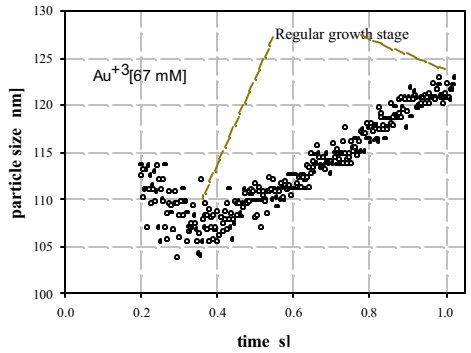

Figure 6: Growth kinetics of gold particles [1].

For similar concentrations in the water phases, the growth process to form particles of about 100 nm, goes for less than 1s, for the aqueous medium process, represented in Figures 5 and 6, to several minutes, for the process with reverse micelles, represented in Figures 7 and 8. Coalescence of micelles after reduction seems to be the limiting step in this process.

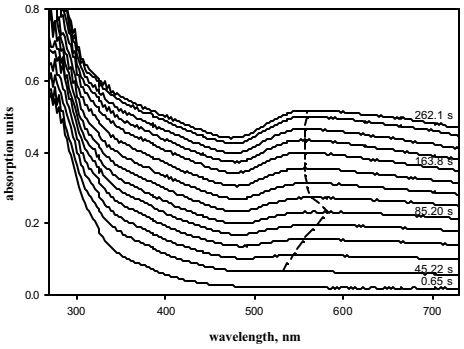

Figure 7: Gold Particle Growth in reverse micelles; Au^{+3} [0.038 mol/l], SO_3^{-2} [0.126 mol/l], $w = [H_2O]/[AOT] = 10$.

In addition, particle size reaches a maximum and then decreases (see Figures 7 and 8). This is apparently due to aggregation of particles that are covered by surfactant, and that easily separate later on.

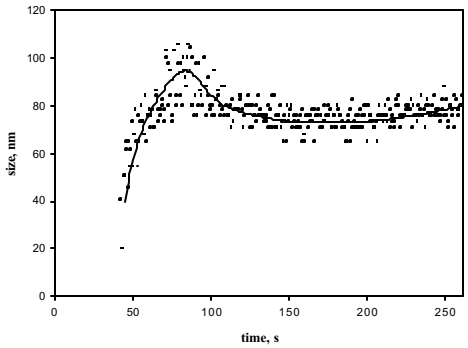

Figure 8: Gold Particle Growth in reverse micelles; Au^{+3} [0.038 mol/l], SO_3^{-2} [0.126 mol/l], w= $[H_2O]/[AOT]$ = 10.

In the particular case indicated on the above figure, the particles reach a final size of about 80 nm. This microemulsion of gold particles remained stable for several weeks.

REFERENCES

1. Murillo, L.E; et al. Computational Nanoscience and Nanotech, 435-438, 2002
2. Vicu a, E.; et al. Nanotech, 3, 191, 2003.
3. Okitsu, K.; et al. Langmuir 17: 7717-7720, 2001.
4. Mandal, M.; et al. Bull. Mater. Science 25: 509-511, 2002.
5. Mandal, M.; et al. Langmuir 18: 7792-7797, 2002.
6. Feldheim, D., and C. Foss Jr., *Metal nano-particles: synthesis, characterization and applications.* Marcel Dekker Inc, New York, 2002.
7. Hainfield, J., and R. Powell. Journal of Histochemistry and Cytochemistry 48: 471-480, 2000.
8. Kreibig, U.; et al. Physical Stat. sol (a) 175:351-367, 1999.
9. Chen, F.; et al. Materials Letters 4325: 1-5, 2003.
10. Liu, S; et al. Langmuir 18: 8350-8357, 2002.
11. Feltin, N., and M.P. Pileni. Langmuir 13: 3927-3930, 1997.
12. Pileni, M.P. Journal of Physical Chemistry 97: 6961-6973, 1993.
13. Petit, C.; et al. Journal of Physical Chemistry (B) 103: 1805-1810, 1999.
14. M.P Pileni. Crystal Research Technology 33: 1155-1186, 1998.
15. Pileni, M.P; et al. Chemical Physics Letters 118: 414-420, 1985.
16. LLai, R.; et al. Journals of Magnetism and Magnetic Materials 163: 243-248, 1996.
17. Sau, K.T.; et al. Journal of Physical Chemistry B. 105: 9266-9272, 2001.
18. Mie, G, Ann. Phys., 25: 377, 1908.
19. Kreibig U. and M. Vollmer, *Optical Properties of Metal Clusters*. Springer, Berlin, 1995
20. Galletto P., Brevet, P., Girault, H., Antoine, R., and M. Broyer. J. Phys. Chem. B, 103: 8706-8710, 1999
21. Logunov S., Ahmadi,T., El-Sayed, M., Khoury, J., and R. Whetten,. J. Phys. Chem. B, 101:3713, 1997.
22. Stephan, L., and M.A. El-Sayed, J. Phys.Chem. B, 103: 4212, 1999
23. Sau T.K., Pal A., Jana N.R., Wang Z.L., and T. Pal., J. Nanoparticle Res., 3: 257, 2001
24. Viera O., *Growing of Gold Nano-particles from Aqueous Solution.* MS thesis, University of Puerto Rico at Mayagüez, 2002.